Identifying spatial and temporal dynamics of proglacial groundwater-surface-water exchange using combined temperature-tracing methods

Tristram, Dominic A; Krause, Stefan; Levy, Amir; Robinson, Zoe P.; Waller, Richard; Weatherill, John

DOI:
10.1086/679757

Document Version
Publisher's PDF, also known as Version of record

Citation for published version (Harvard):
Tristram, DA, Krause, S, Levy, A, Robinson, ZP, Waller, R & Weatherill, J 2015, 'Identifying spatial and temporal dynamics of proglacial groundwater-surface-water exchange using combined temperature-tracing methods', *Freshwater Science*, vol. 34, no. 1, pp. 99-110. https://doi.org/10.1086/679757

Identifying spatial and temporal dynamics of proglacial groundwater–surface-water exchange using combined temperature-tracing methods

Dominic A. Tristram[1,3], Stefan Krause[1,4], Amir Levy[2,5], Zoe P. Robinson[2,6], Richard I. Waller[2,7], and John J. Weatherill[2,8]

[1]School of Geography, Earth and Environmental Sciences, University of Birmingham, Birmingham B15 2TT UK
[2]Research Institute for the Environment, Physical Sciences and Applied Mathematics (EPSAM). Keele University, Keele, Staffordshire ST5 5BG UK

Abstract: The effect of proglacial groundwater systems on surface hydrology and ecology in cold regions often is neglected when assessing the ecohydrological implications of climate change. We present a novel approach in which we combined 2 temperature-tracing techniques to assess the spatial patterns and short-term temporal dynamics of groundwater–surface-water exchange in the proglacial zone of Skaftafellsjökull, a retreating glacier in southeastern Iceland. Our study focuses on localized groundwater discharge to a surface-water environment, where high temporal- and spatial-resolution mapping of sediment surface and subsurface temperatures (10–15 cm depth) were obtained by Fiber-Optic Distributed Temperature Sensing (FO-DTS). The FO-DTS survey identified temporally consistent locations of temperature anomalies at the sediment–water interface, indicating distinct zones of cooler groundwater upwelling. The high-resolution FO-DTS surveys were combined with calculations of 1-dimensional groundwater seepage fluxes based on 3 vertical sediment temperature profiles, covering depths of 10, 25, and 40 cm below the lake bed. The calculated groundwater seepage rates ranged between 1.02 to 6.10 m/d. We used the combined techniques successfully to identify substantial temporal and spatial heterogeneities in groundwater–surface exchange fluxes that have relevance for the ecohydrological functioning of the investigated system and its potential resilience to environmental change.
Key words: proglacial groundwater, groundwater–surface-water exchange, Fiber-Optic Distributed Temperature Sensing, seepage flux, glacial retreat, ecohydrology, Iceland

Groundwater flow and storage influence the timing (Tague and Grant 2009) and magnitude (Clow et al. 2003, Baraer et al. 2009) of surface-water discharge in glaciated catchments. Groundwater-fed proglacial rivers and lakes can affect the wider catchment hydrology (Mellina et al. 2002, Richards et al. 2012), biogeochemistry (Goodman et al. 2010, 2011), and ecology (Roy and Hayashi 2009), often causing enhanced biodiversity in streams directly affected by ground water (e.g., Milner and Petts 1994, Ward et al. 1999, Malard et al. 1999, Brown et al. 2007b, Crossman et al. 2011, 2013, Roy et al. 2011, Jacobsen et al. 2012). Climate change, including glacial retreat and changes in precipitation patterns and melt timing, is projected to significantly affect proglacial groundwater systems with, for instance, expected increases in groundwater contributions and changes to hydrochemical conditions and nutrient cycling (Milner et al. 2009, Rutter et al. 2011, Blaen et al. 2013). These projected changes are expected to have significant effects on ecosystem functioning and biodiversity (e.g., Brown et al. 2007a, Milner et al. 2009). In contrast to the well investigated effect of climate change on proglacial surface-water systems (e.g., Singh and Bengtsson 2005, Huss et al. 2008, Mark 2008, Casassa et al. 2009, Stewart 2009, Nolin et al. 2010), potential interactions with proglacial groundwater systems have not been investigated in similar detail (Piotrowski 2007). To understand the potential responses and resilience of proglacial groundwater systems to climate change, the processes controlling the spatially and temporally dynamic interactions between ground water and proglacial rivers and lakes have to be identified

E-mail addresses: [3]Present address: WorleyParsons, 2nd Floor, Bull Wharf, Redcliff Street, Bristol, BS1 6QR, UK, datristram@gmail.com
[4]s.krause@bham.ac.uk; [5]a.levy@keele.ac.uk; [6]z.p.robinson@keele.ac.uk; [7]r.i.waller@keele.ac.uk; [8]j.j.weatherill@keele.ac.uk

DOI: 10.1086/679757. Received 3 October 2013; Accepted 28 September 2014; Published online 9 January 2015.
Freshwater Science. 2015. 34(1):99–110.

(Cooper et al. 2002, McClymont et al. 2012, Langston et al. 2013).

Regional hydrogeological conditions play a key role in controlling the magnitude and spatial patterns of groundwater–lake exchange (Hood et al. 2006), so the magnitude and patterns of groundwater–lake exchange can vary substantially because of the heterogeneity of proglacial hydrogeological properties. Previous studies in different proglacial environments have identified both negligible groundwater–lake exchange (e.g., Michel et al. 2002, Winter 2003) and groundwater–lake exchange that significantly affected lake water balance (Campbell et al. 2004, Gurrieri and Furniss 2004, Hood et al. 2006, Roy and Hayashi 2008, Kidmose et al. 2013, Meinikmann et al. 2013).

Spatial heterogeneity in proglacial groundwater–surface-water interactions has been related to a variety of geomorphological and hydrogeological controls (Brown et al. 2006, Robinson et al. 2008, Rutter et al. 2011), including the internal heterogeneities of moraine structures (Roy and Hayashi 2009, Langston et al. 2011). On the other hand, temporal variability in groundwater–surface-water exchange in proglacial systems frequently is controlled by the diurnal, seasonal, and annual variability of melt and precipitation (e.g., Brown et al. 2006). Predicted long-term decrease of meltwater discharge, as a result of glacial retreat, is projected to affect proglacial groundwater–surface-water exchange (Brown et al. 2007a).

Identification and understanding of the organizational principles of spatial and temporal dynamics of proglacial groundwater–surface-water exchange fluxes is paramount for assessing potential effects of glacial retreat on proglacial rivers and lakes of high hydrological relevance (e.g., Milner et al. 2009). Methods for monitoring and quantifying groundwater–surface-water exchange have improved substantially (Kalbus et al. 2006, Fleckenstein et al. 2010, Krause et al. 2011a, b, c), but the heterogeneity of hydrogeological conditions (e.g., Roy and Hayashi 2008, 2009) and logistic difficulties can impede the tracing of groundwater–surface-water exchange using traditional hydrogeological methods, such as techniques based on Darcy's Law (Lautz 2010, Shaw et al. 2013).

However, the recent advances in the application of heat as a tracer for the direction and magnitude of groundwater–surface-water exchange fluxes provide promising tools for quantifying groundwater contributions to proglacial surface-water systems (Westhoff et al. 2007, Constantz 2008, Anibas et al. 2009, Hatch et al. 2010, Lautz 2010, Briggs et al. 2012). In particular the development of Fiber-Optic Distributed Temperature Sensing (FO-DTS) enables monitoring of groundwater–surface-water exchanges at unprecedented spatial and temporal scales (e.g., Selker et al. 2006a, b, Tyler et al. 2009, Krause et al. 2012, Krause and Blume 2013, Rose et al. 2013). FO-DTS measures temperature by analyzing the offset in the backscatter of Raman Stokes and antiStokes signals from a 10-ns light pulse that is applied to a fiber-optic cable (Selker et al. 2006 a, b, Tyler et al. 2009). The method provides high spatial- and temporal-resolution thermal mapping at the sediment–surface-water interface, where the identified temperature anomalies can be used to locate groundwater upwelling (Lowry et al. 2007, Westhoff et al. 2011, Krause et al. 2012, Blume et al. 2013, Briggs et al. 2013, Krause and Blume 2013).

Our objectives were to identify groundwater–surface-water exchange fluxes in a proglacial lake adjacent to a retreating glacier in southeastern Iceland. We combined different temperature-tracing methods to investigate organizational principles of exchange fluxes between the proglacial lake and associated groundwater system. Our specific objectives were to: 1) map temperature patterns of lake sediment pore water and the sediment–lake-water interface in high spatial and temporal resolution using Fiber-Optic Distributed Temperature Sensing (FO-DTS) technology, 2) use temperature anomalies at the groundwater–lake-bed interface to infer groundwater–lake exchange flow patterns and to delineate groundwater discharge zones to the proglacial lake, 3) calculate 1-dimensional vertical groundwater seepage fluxes at selected upwelling zones using high-resolution time series of sediment porewater temperature profiles.

METHODS

Skaftafellsjökull proglacial zone

Skaftafellsjökull is a temperate valley glacier in southeastern Iceland. Most of its ice is sourced from the Vatnajökull ice cap (Tweed et al. 2005, Cook et al. 2010) (Fig. 1A). The glacial margin is ~3 km wide, 120 m asl, and borders a coastal plain. Skaftafellsjökull melt water feeds the Skaftafellsá River (Marren and Toomath 2013) (Fig. 1B). The glacier has retreated ~1.5 km since monitoring began in the 1940s (IGS 2013). Seismic surveys from the proglacial zone of the glacier Svínafellsjökull (east of Skaftafellsjökull) suggest unconsolidated sediment depths of 80 to 150 m (Guðmundsson et al. 2002). As identified by stable isotope studies in nearby Skeiðarársandur, the dominant sources of shallow groundwater recharge are precipitation and glacial melt (Robinson et al. 2009a, b). The same study revealed that the signature of ice melt diminishes with increasing distance from the glacier. The mean annual precipitation (1995–2012) at the study area was 1595 mm/y, with average temperatures of 5.15°C (IMO 2013).

The field site is ~1 km south of the current Skaftafellsjökull margin (Fig. 1C). Field work for our study focused on Swan Lake (lat 64°00 42.84 N, long 16°54 20.77 W). The lake was ~30 × 50 m with a circumference of ~150 to 160 m (Fig. 1C). The northern, southern, and eastern boundaries of the lake are confined by moraines that are ~3 m high. No outlet stream was associated with Swan Lake. The deepest section of the lake is on its eastern side (~2.5 m depth) and is underlain by ~0.5 m of clay and

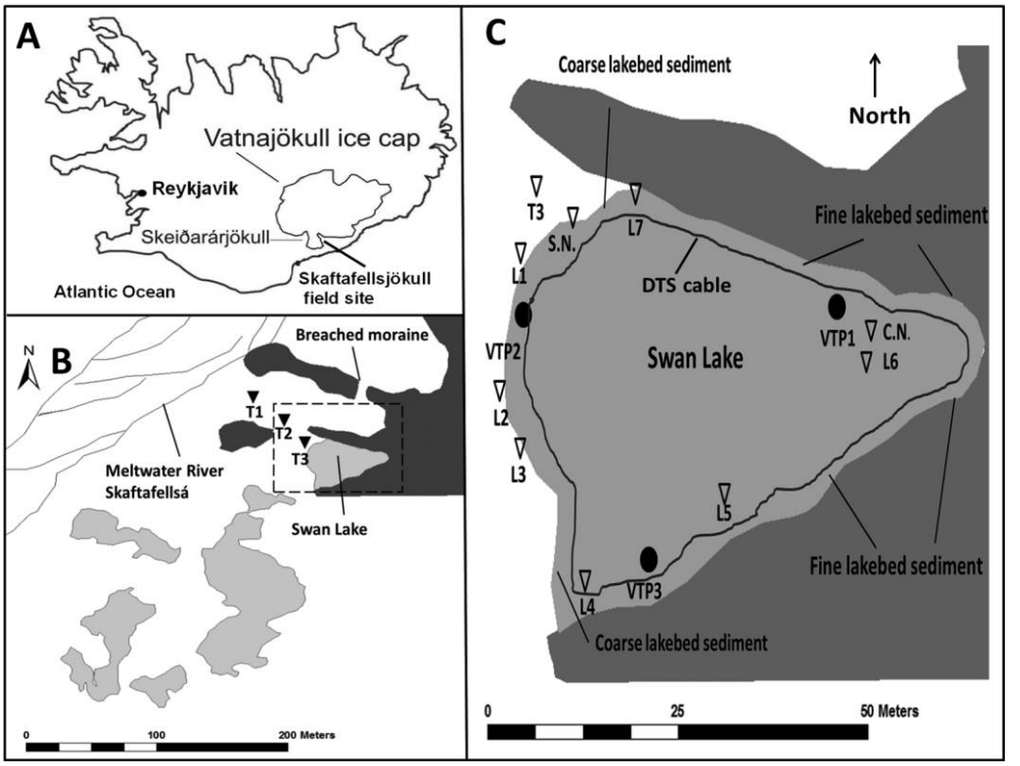

Figure 1. Map of the field site in Iceland (A), the proglacial zone of the Skaftafellsjökull glacier (B), and details of study area Swan Lake (dashed box in B, C). Swan Lake has no outlet stream. Inverted triangles denote piezometers, and circles denote the location of the Vertical Temperature Profiles (VTP). The location and deployment of the Fiber-Optic Distributed Temperature Sensor (FO-DTS) cable is shown as a black curve. Clay nest (C.N.) and Sand Nest (S.N.) denote 12-mm diameter piezometer nests within the respective sediment. L1–7 denote piezometers with internal diameter of 12 mm. T1–3 denote shallow boreholes with internal diameter of 22 mm.

boulders. Substantial sediment heterogeneity was observed around the lake. The eastern side is underlain by fine sediment and the western side by coarse sand and gravel (Table 1).

Monitoring of groundwater levels

We installed piezometers for monitoring groundwater levels in June 2012 and monitored between 18 and 29 June 2012. The piezometer network covered the lake perimeter and locations between Swan Lake and the River Skaftafellsá to assess groundwater–lake exchange (Fig. 1C). Piezometers were designed from polyvinyl chloride (PVC) tubes (12–22 mm internal diameter) with 500-mm-long screened sections. We installed the piezometers to a depth of ~2 m below ground level with drive-point techniques (Krause et al. 2011b) and measured piezometric heads twice a day with a manual Solinst graduated electric contact meter (dip meter; Solinst, Georgetown, Canada), with an accuracy of ±3 mm (Krause et al. 2011b). We monitored the T1–T3 transect between the river Skaftafellsá and Swan Lake (Fig. 1C) with Solinst Levelogger Junior pressure transducers at 5-min intervals. We set up a stilling

Table 1. Particle size distribution at each vertical temperature profile (VTP) location. VTP 2 contains data from only 10 cm depth. D_{10}, D_{50}, and D_{90} = 10th, 50th, and 90th percentiles of particle size (mm).

Particle size (μm)	VTP 1 10 cm	VTP 1 25 cm	VTP 1 40 cm	VTP 2 10 cm	VTP 3 10 cm	VTP 3 25 cm	VTP 3 40 cm
D_{10}	4.93	4.21	4.43	15.37	5.12	10.08	11.68
D_{50}	21.91	19.16	20.00	175.70	22.43	42.47	50.63
D_{90}	54.58	45.22	51.56	1021.00	57.28	155.40	145.90

well equipped with the same device to record river levels. The piezometers were surveyed with a Leica Total Station (Leica, Milton Keynes, UK).

FO-DTS

We applied a Sensornet Halo FO-DTS, which measures temperature at high precision (0.05°C) at 30-s intervals with a sampling resolution of 2 m (http://www.sensornet.co.uk/images/technology/halo/download8a2d.cfm.pdf). We deployed a 500-m-long 2-channel fiber-optic cable (Bru-Outdoor; Brugg/CH, Brugg, Switzerland) within ~2 m of the lake circumference (Fig. 1C).

In most previous FO-DTS studies (with the exception of Lowry et al. 2007, Krause et al. 2012, Krause and Blume 2013) fiber-optic cables were deployed at the sediment surface, effectively measuring surface water-column temperatures. We installed the fiber-optic cable at 2 depths, on top of the sediment and ~10 cm within the lake-bed sediment. This design allowed direct comparison of temperatures in the lake-bed sediment and at the sediment–water interface, where they are potentially more intensely influenced by surface-water temperatures. We installed the buried cable by hand, and spot checks indicated that the deployment depth remained constant during the course of the experiment. The FO-DTS set-up used alternating single-ended measurements in clockwise and anticlockwise directions that we combined in 2-way single-ended averaging mode as described by Krause and Blume (2013). We did the dynamic temperature calibration in a calibration bath (containing meltwater from the river) where temperature was monitored continuously. We synchronized the time intervals of the calibration-bath measurements with the FO-DTS monitoring intervals.

Estimation of seepage rates by vertical temperature profiles

The method for calculating 1-dimensional vertical seepage fluxes is based on a continuous time series of vertical lake-bed temperature profiles, assuming purely vertical flow, sinusoidal temperature fluctuations, and no thermal gradient at the lake bed (Hatch et al. 2006, Lautz 2010). Violations of these assumptions were tested previously by Lautz (2010), who found the model to be robust.

We monitored vertical temperature profiles (VTP) from the lake-bed sediment with automatic HOBO thermistors (U12-008 4 Ch Industrial Data Logger, Tempcon Instrumentation Ltd., West Sussex, UK) set to record at 5-min intervals. Each VTP included depths of 10, 25, and 40 cm. The thermistor profiles followed the design of Krause et al. (2011a). Four-cm screened sections at the bottom of the metal tube allowed groundwater infiltration and direct contact with the temperature sensor at specified depths. We installed VTP 1 in fine sediment, whereas we installed VTPs 2 and 3 in coarser sediment (Fig. 1C, Table 1). We calculated 1-dimensional heat transport, based on conduction, advection, and dispersion as (Hatch et al. 2006, Keery et al. 2007, Lautz 2010):

$$\frac{\partial T}{\partial t} = \kappa_e \frac{\partial^2 T}{\partial z^2} - \frac{q}{\gamma}\frac{\partial T}{\partial z} \qquad \text{(Eq. 1)}$$

where T is temperature (°C), which is a variant of time (t; s) and depth (z; m), κ_e is effective thermal diffusivity (m^2/s), q is vertical seepage flux (m/s), and γ the ratio of heat capacity of the sediment–water matrix in the lake bed to the water heat capacity (Lautz 2010). Groundwater fluxes (q) (m/s) (Lautz 2010) were calculated as:

$$q = \frac{\rho c}{\rho c_w}\sqrt{\alpha - 2\frac{\Delta\varphi 4\pi\kappa_e^2}{P\Delta z}} \qquad \text{(Eq. 2)}$$

where ρc and ρc_w are heat capacity of sediment–water matrix and water respectively (J m^{-3} $°C^{-1}$), Δz = difference in depth between 2 measurement points in the lake bed (m), P = period of temperature signal (s), and $\Delta\varphi$ = lag time (h) between the maximum correlation of temperature between the uppermost and lower temperature sensors. We calculated the lag time from the Cross Correlation Function (CCF) between the different temperature sensors (Hannah et al. 2009, Krause et al. 2011a, b) with software by Wessa (2012). We obtained ranges of parameter values for Eqs 1–4 from the literature (Table 2).

We calculated the α perimeter as:

$$\alpha = \sqrt{v^4 + \left(\frac{8\pi\kappa_e}{P}\right)^2} \qquad \text{(Eq. 3)}$$

where v is the velocity of the thermal front (m/s). We used the equation 'speed = distance/time' to calculate speed, where distance is the depth to the logger sensor and time is the lag time obtained from the CCF data for that particular sensor. We calculated κ_e as:

$$\kappa_e = \frac{\lambda_e}{\rho c} \qquad \text{(Eq. 4)}$$

where λ_e is the effective thermal conductivity (J s^{-1} m^{-1}), and ρc is the heat capacity of the saturated sediment–water matrix (J m^{-3} $°C^{-1}$) (Hatch et al. 2006). We obtained λ_e from studies in streams with fine and coarse sediment (Lautz 2010) and ρc from data published by Lapham (1989).

Analysis of damping depths of diurnal temperature oscillations

The damping depth (d) represents the amplitude decrease in the strength of the temperature signal with increas-

Table 2. Parameters used in Eqs 1–4 (Hillel 2004, Lautz 2010) to calculate seepage fluxes based on parameters for fine and coarse sediment.

Sediment property	Sediment size	Units	Value used in the equation	Reference(s)
Effective thermal conductivity (λ_e)	Fine	J/(s m °C)	0.84	Lautz 2010
	Coarse		1.67	
Heat capacity of saturated sediment–fluid system (ρc)	Fine	J/(m^3 °C)	3.6×10^6	Lapham 1989
	Coarse		3.1×10^6	
Heat capacity of water (ρc_W)	Fine	J/(m^3 °C)	4.2×10^6	Lautz 2010
	Coarse			
Effective thermal diffusivity (κ_e)	Fine	m^2/s	2×10^{-7}	Lapham 1989, Lautz 2010
	Coarse		5×10^{-7}	

ing depth from the water–sediment interface. The damping depth is the depth at which temperature oscillation will naturally attenuate without taking into account any effects from advective processes, such as water upwelling or downwelling. We calculated the damping depth as (Hillel 1998):

$$d = 0.5\left(\frac{D_h \tau}{\pi}\right) \quad \text{(Eq. 5)}$$

where D_h is thermal diffusivity and τ is the period of oscillation. Thermal diffusivity is calculated by multiplying thermal conductivity and volumetric specific heat, by which the parameters depend upon water content, porosity, and bulk density (Hillel 2004, Krause et al. 2011a, b).

RESULTS AND DISCUSSION

Meteorological conditions

Air temperatures during the research period (1900 h 20 June–2300 h 31 July 2012) at the field site ranged between 1.10 and 22.80°C (average = 11.24°C) with diurnal fluctuations from 5.90 to 18.50°C (IMO 2013) (Fig. 2). During the 12-month period preceding the investigations, mean monthly precipitation exceeded long-term averages during the autumn and winter months by up to 150 mm. In contrast, precipitation from April–August 2012 was sig-

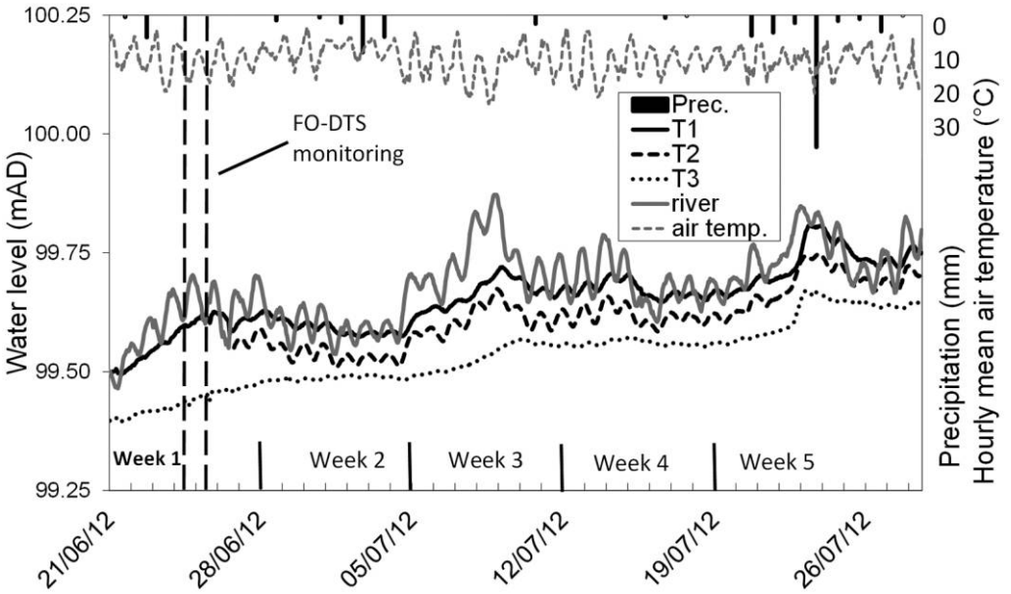

Figure 2. Hourly meltwater levels of river Skaftafellsá (meters above datum) and hydraulic heads at boreholes T1–3, and mean hourly air temperature and total daily precipitation at the site during the study period. The vertical dashed lines during week 1 represent the duration of the Fiber-Optic Distributed Temperature Sensor study. Dates are formatted dd/mm/yy.

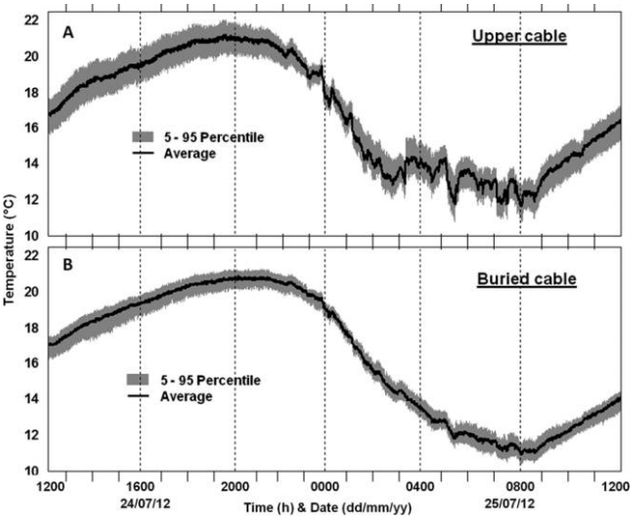

Figure 3. Mean and 5th and 95th percentile temperatures (T) for lake-bed sediment (upper cable) (A) and 10 cm depth within the lake-bed sediment (buried cable) (B) recorded during the Fiber-Optic Distributed Temperature Sensor (FO-DTS) temperature surveys.

nificantly below the long-term monthly average. Precipitation during the investigation occurred solely as rainfall (total = 79.8 mm) with the highest daily rainfall on 23 July 2012 (33.3 mm) (Fig. 2).

Surface and groundwater levels

Low precipitation during spring and summer of 2012 coincided with declining lake water levels at Swan Lake and other lakes at the field site. At the start of the study, ~0.30-m-high exposures of dried lake banks illustrated the rapid response of the lake–groundwater system to antecedent dry conditions and showed that lake and groundwater levels were sensitive to changes in local precipitation.

Diurnal oscillations of the River Skaftafellsá water levels were recorded during the study (Fig. 2). These oscillations suggested a probable relationship between diurnal air-temperature oscillations and glacial meltwater volumes. This relationship was supported by an increase in air temperature and river water level between 7 and 9 July 2012. Furthermore, a decrease in air temperature from 29 July 2012 onward resulted in a decrease in water level of ~0.23 m (Fig. 2).

Spatial patterns of groundwater discharge

The 24-h FO-DTS monitoring revealed a clear diurnal pattern of temperatures at both the sediment–water interface and at ~10 cm depth within the lake-bed sediment (Fig. 3A, B). During the 24-h FO-DTS monitoring, average temperatures at the sediment–water interface ranged between ~11.5 and 21°C (range = 9.5°C), whereas averaged spatial temperatures 10 cm within the sediment varied between ~11 and 20°C (range = 9°C) (Fig. 3A, B). Temperatures at the sediment–water interface generally were less stable than at 10 cm within the sediment. This difference was especially pronounced during the temperature recession between 2200 and 0800 h when average temperatures at the sediment–water interface varied by up to 2.5°C in contrast to <1°C 10 cm within the sediment. The difference between 5th and 95th percentiles of temperature was ~2°C at the sediment–water interface and <1°C 10 cm within the sediment (Fig. 3A, B). This damping of the spatial temperature patterns at depth indicates that existing surface-water signals were propagating into the sediment where they were less pronounced than in the lake. FO-DTS mapping of sediment–water-interface and subsurface temperatures highlighted distinct zones of colder-than-average temperatures, which appeared consistently in the northern, and most notably, eastern areas of the lake (Fig. 4). Their locations at the sediment–water interface and at 10 cm within the sediment were consistent throughout the FO-DTS survey (Figs 4, 5). These observations were supported by a comparison of the deviation of local temperatures from the spatial average (Fig. 6A, B). Groundwater temperatures at the site generally were lower than lake temperatures. Thus, spatial patterns of cold-spots can be attributed to groundwater upwelling (Sebok et al. 2013).

The greater local deviations from the spatial mean in the sediment than at the sediment–water interface) (Fig. 6A, B) indicate a rapid dissipation of the colder ground water within the surface water column and coincide with previous findings by Krause et al. (2012) and Krause and Blume (2013). These results suggest that FO-DTS provides a use-

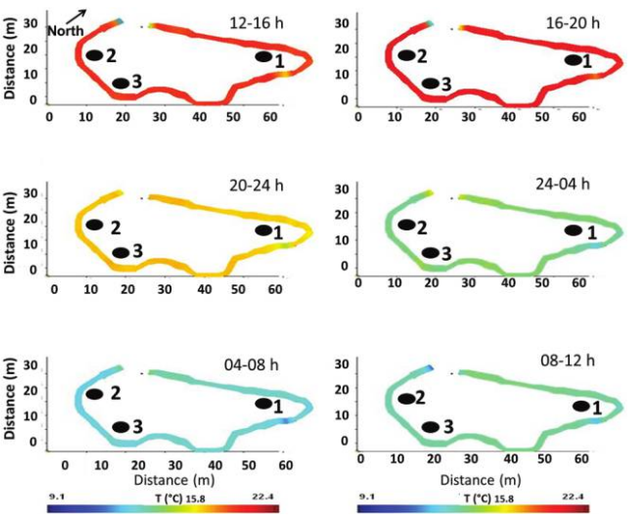

Figure 4. Fiber-Optic Distributed Temperature Sensor (FO-DTS) measurements (4-h means) at the lake-bed–surface-water interface (upper cable). Locations of vertical temperature profiles (VTPs) are identified by numbered black circles.

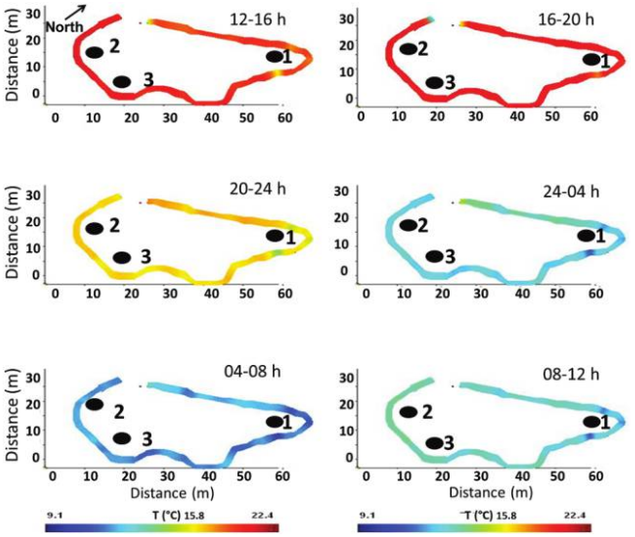

Figure 5. Fiber-Optic Distributed Temperature Sensor (FO-DTS) measurements (4-h means) at 10 cm depth within the lakebed sediment (buried cable). Locations of vertical temperature profiles (VTPs) are identified by numbered black circles.

ful mean of identifying potential hotspots of groundwater seepage into proglacial lakes.

Dynamics of VTPs

Sediment temperatures exhibited strong diurnal oscillations that attenuated with depth at all 3 locations, indicating an increase in porewater thermal stability with depth. The strongest temperature oscillations were observed at 10 cm depth, whereas oscillations at 40 cm depth were negligible (Fig. 7A–C). Lower air temperatures from 14 to 23 July 2012 (Fig. 2) corresponded with lower porewater temperatures at all locations, whereas higher air temperatures corresponded with higher porewater temperatures across the vertical profile (Fig. 7A–C). For example, the average temperature difference between 10 and 25 cm at VTP 1 was 1.06°C but increased to ~2°C during warmer periods (e.g., 25 June). Conversely, the temperature difference decreased to ~0.2°C during cooler periods (e.g., 4 July) (Fig. 7A–C).

The CCF values generally were high except that VTP 1 was 0.734 during week 3 (this value is not considered low; Table 3). On several occasions (weeks 1, 3, and 4), the lag time of signal propagation between 10 and 25 cm depth was higher at VTP 1 than at VTP 2 and 3 (Table 3). The strongest diurnal oscillations occurred at VTP 2, along with the smallest differences in mean porewater temperature between 10 and 25 cm (0.25°C) and between 25 and 40 cm depth (1.12°C) (Fig. 7B). At VTP 2, oscillating porewater temperatures at 10 and 25 cm depth were similar throughout the study and temperatures were nearly identical during the daily minimum (Fig. 7B). The similarity of temperature dynamics observed at different depths at VTP 2 probably arose from the coarser subsurface sediment at this location than at VTP 1 and 3 (Table 1). Higher thermal conductivity of the coarser sediment would support deeper propagation of diurnal oscillation into the subsurface. The smallest diurnal oscillations occurred at VTP 3 where absolute temperatures generally were higher than at VTP 1 and 2. Porewater temperatures at VTP 3 showed the smallest amplitude difference in mean daily oscillation between the different depths. Mean amplitudes were 0.83°C at 10 cm, 0.43°C at 25 cm, and 0.16°C at 40 cm (Fig. 7C). At VTP 1, the mean amplitude of diurnal porewater temperature oscillations at 10 cm depth was 1.06°C. It then attenuated with depth to ~0.49°C at 25 cm depth and ~0.23°C at 40 cm depth (Fig. 7A). Greater attenuation of absolute temperature and diurnal oscillations occurred between 25 and 40 cm, indicating greater groundwater influence and reduction of atmospheric forcing with increasing depth.

Field data comparison of damping depths

The calculated damping depths (Eq. 5) for sandy and clayey sediment were 0.62 and 0.53 m, respectively. Thus, temperature signals for sandy conditions (VTP 2) were expected to be attenuated at 9 cm deeper than in clayey conditions (VTP 1 and 3). Both calculated damping depths exceeded the depth of the deepest temperature logger (40 cm) in the lake bed. However, the negligible daily oscillations recorded at 40 cm depth for each location (Fig. 7A, C) indicate signal attenuation at depths shallower than calculated, strongly suggesting additional attenuation of temperature propagation by upwelling groundwater.

Quantification of groundwater seepage fluxes

The calculated 1-dimensional vertical seepage fluxes ranged between 1.02 and 6.10 m/d (Table 3) and highlight the importance of groundwater discharge to the lake. Seep-

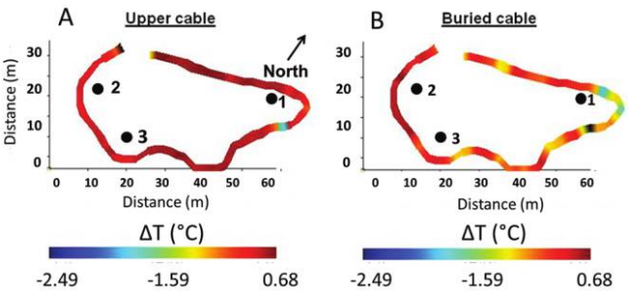

Figure 6. Local deviations (averaged over 24 h) of Fiber-Optic Distributed Temperature Sensor (FO-DTS) measurements from the spatial mean temperature (ΔT) at the lake-bed–surface-water interface (upper cable) (A) and 10 cm within the lake-bed sediment (buried cable) (B). Locations of vertical temperature profiles (VTPs) are identified by numbered black circles.

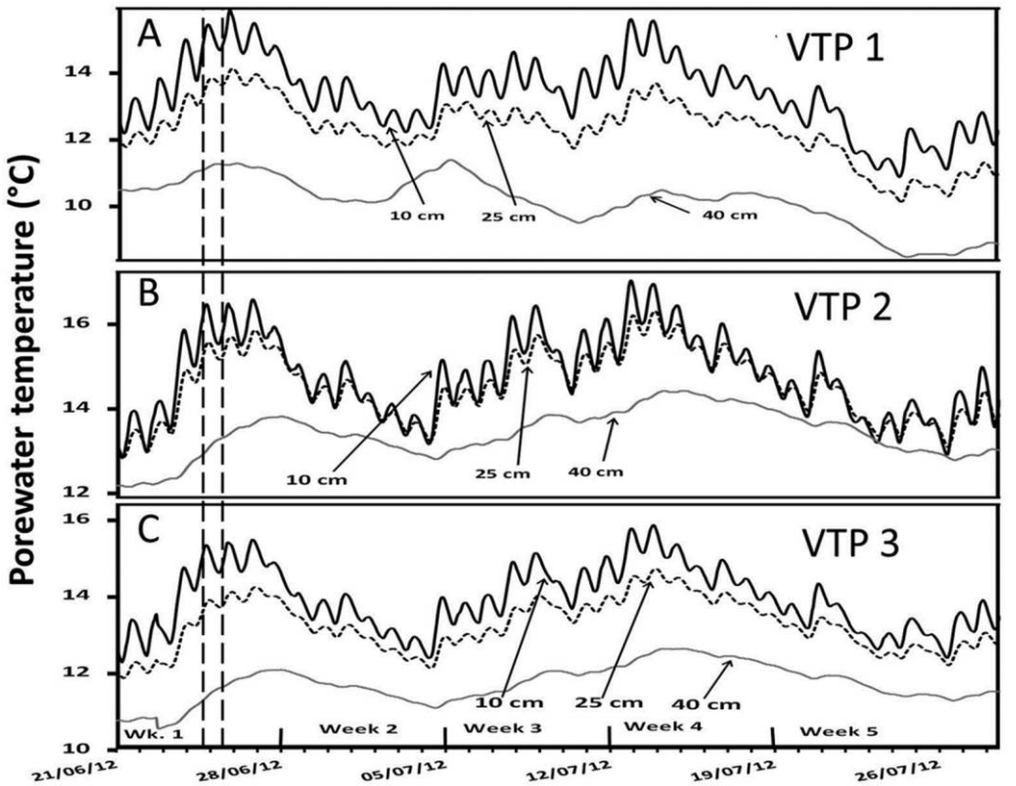

Figure 7. Vertical porewater temperature profile (10, 25, 40 cm depth) recorded at vertical temperature profile (VTP) 1 (A), 2 (B), and 3 (C). The location of each VTP is shown in Fig. 1C. The vertical dashed lines during week 1 represent the duration of the Fiber-Optic Distributed Temperature Sensor (FO-DTS) study. Dates are formatted dd/mm/yy.

age fluxes for VTP 2 were calculated using both sand and clay parameters (Eqs 2 and 4), but VTP 1 and 3 were calculated for clay only. The lowest seepage flux was identified at VTP 1 (1.02 m/d during week 4) when fluxes at VTP 2 and 3 were higher (Table 3). However, during weeks 2 and 5, fluxes at this location were the same as calculated for VTP 2 and 3 (Table 3).

Seepage at VTP 1 significantly increased by 4.58 m/d between weeks 1 and 2 (Table 3). A similar increase was observed at VTP 3. This increase might have been the re-

Table 3. Calculated lag times, cross-correlation function CCF), and seepage fluxes for the vertical temperature profiles (VTPs).

Variable	Week 1 (21–28 June)	Week 2 (29 June–6 July)	Week 3 (6–13 July)	Week 4 (13–19 July)	Week 5 (20–28 July)
Lag time (h)					
V TP 1 (25 cm)	2	0.5	2	3	2
VTP 2 (25 cm)	0.5	0.5	1	2	2
VTP 3 (25 cm)	1	0.5	1	2	2
CCF					
VTP 1 (25 cm)	0.969	0.923	0.734	0.948	0.926
VTP 2 (25 cm)	0.980	0.968	0.941	0.973	0.943
VTP 3 (25 cm)	0.969	0.969	0.912	0.946	0.926
Seepage flux (m/d)					
VTP 1	1.52	6.10	1.52	1.02	1.52
VTP 2 (sand)	6.10	6.10	3.05	1.52	1.52
VTP 2 (clay)	6.10	6.10	3.05	1.52	1.52
VTP 3	3.05	6.10	3.05	1.52	1.52

sult of higher rates of groundwater discharge subsequent to increased rainfall. At VTP 1 and 3, temperature propagation was slightly attenuated during week 2 (Fig. 7A, C), a result supporting the assumption that cooler groundwater buffers heat conduction from the surface during periods of enhanced groundwater upwelling. However, cooler air temperatures during this week also may have contributed to these patterns. Seepage fluxes at all locations declined in weeks 2 to 5, with the greatest decrease (4.58 m/d) occurring at VTP 1 (Table 3), possibly because low rainfall during weeks 2 to 4 reduced groundwater recharge and subsequent groundwater seepage into the lake.

FO-DTS-identified hotspots of groundwater upwelling and quantified fluxes based on the 3 temperature profiles did not match on all occasions. The FO-DTS survey identified a strong temperature anomaly in the northeastern section of the lake shore (Figs. 4, 5), indicating discrete, spatially confined hotspots of groundwater discharge, but VTP 1 in the near vicinity did not detect increased groundwater fluxes at this location. During several weeks (weeks 1, 3, 4), fluxes at VTP 1 were lower than at the 2 other VTP locations (Table 3). This result might be further indication of the high spatial heterogeneity in sediment properties resulting in highly variable spatial patterns of groundwater–surface-water exchange. The location of VTP 1 for the temperature-profile-based flow calculations was several meters from the FO-DTS-identified thermal anomaly at the northeastern lake section. Thus, the interpretation is plausible, given that temperature anomalies along the fiber-optic cable occurred at similar spatial scales as the distance between the cable and VTP 1. However, uncertainties in the data interpretations have to be considered. These uncertainties include limited knowledge of spatial variability in sediment characteristics and, as a result, low sensitivity of the temperature-based flow calculations to changes in properties of the chosen thermal material.

Limitations and recommendations for future work

We combined FO-DTS and calculation of 1-dimensional vertical seepage fluxes to assess groundwater–surface-water exchange at different temporal and spatial scales. FO-DTS identified spatial and temporal variability in groundwater–surface-water interactions at high resolution. Calculation of seepage fluxes allowed us to quantify exchange fluxes over longer periods of several weeks/months. The understanding gained is important for further studies of the response and resilience of groundwater-dependent environments to the projected changes of climate change and glacial retreat.

The combination of applied methods helped to improve mechanistic understanding of the process at different scales. Our results show that the limitations of the methods must be considered when interpreting results. Our interpretation that groundwater was discharged to the proglacial lake was based on the assumption of 1-dimensional vertical fluxes (Hatch et al. 2006). We did not consider lateral fluxes, which cannot be excluded in an environment with such high sediment heterogeneity, in the analyses.

The fact that FO-DTS-identified upwelling hotspots in the northeastern part of the lake could not be verified by the nearby flow calculations at VTP 1 may indicate that even though the applied methods improved the spatial representation of groundwater–surface-water exchange in the research area, the experimental design was not fully successful in capturing the small-scale spatial variability of groundwater upwelling into the lake. More detailed investigations of spatial heterogeneity in lake-sediment properties, associated with a denser network of vertical-flow estimations and a closer alignment of horizontal FO-DTS and vertical temperature profiling methods have the potential to further improve our knowledge of organizational principles of groundwater–lake exchange. Estimation of seepage rates based on only 3 monitoring locations limits detailed upscaling for the entire lake–groundwater interface because sediment heterogeneities and variation in thermal properties can have significant effects on seepage rates (e.g., Krause et al. 2011a, Blume et al. 2013). Moreover, the short period of FO-DTS surveying (24 h) compared to 5 wk of vertical seepage flux monitoring may have affected the comparability of the surveys. New developments in FO-DTS technologies with reduced power demands and adjusted calibration options will enable longer surveys in remote regions, and the combination of horizontal and vertical profile FO-DTS surveys (Briggs et al. 2013) provide promising techniques for future temperature tracing of groundwater–lake interfaces.

Conclusions

FO-DTS monitoring identified substantial spatial and temporal heterogeneity in groundwater discharge into the investigated proglacial lake, with discrete locations of cold groundwater upwelling in the eastern and northern areas of the lake. Calculated seepage fluxes, based on porewater temperature profiles, varied between 1.02–6.10 m/d. Even during the short observation period, substantial temporal variability in groundwater fluxes was observed. This variability might be attributable to changes in groundwater recharge caused by precipitation and meltwater river–aquifer exchange.

Our successful combination of FO-DTS and vertical temperature profiling provided mechanistic understanding of the spatial and temporal patterns of proglacial groundwater–lake exchange. Integration of both heat-tracing methods supported development of a conceptual model of groundwater–surface-water exchange fluxes at the field site and provided evidence of the capacity of the application of both methods combined. Our study highlighted significant potential for ensuring a closer alignment of both methods, which should lead to a better representation of the small-scale variability of groundwater–lake ex-

change in the investigated system. The improved conceptual understanding and, in particular, the field validation of the combined heat-tracing methods provide a valuable tool for future investigations of proglacial lake systems that could be used to examine long-term changes in glacial and pluvial groundwater recharge.

ACKNOWLEDGEMENTS

We thank the anonymous referees, Alan Fryar (University of Kentucky), and Associate Editor Steve Wondzell for constructive reviews that helped to improve the paper. We gratefully acknowledge the Royal Geographical Society with the Institute of British Geographers (RGS-IBG) for the support for field work through the 2012 Postgraduate Research Award, grant number PRA 26.12. We thank the Research Institute for the Environment, Physical Sciences and Applied Mathematics (EPSAM) at Keele University for their support; the Icelandic Glaciological Society and the Icelandic Meteorological Office (IMO) for their kind provision of data; Regina Hreinsdóttir, Gudmundur Ogmundsson, and the rest of the staff at the Skaftafell Visitor Centre (Vatnajökull National Park, Iceland) for their help with fieldwork logistics; Gunnar Bjarki Rúnarsson (of Byko, Selfoss), Olafur Tryggvi Magnusson, and Ian C. Wilshaw (Keele University) for their help with the logistics for field work in Iceland.

LITERATURE CITED

Anibas, C., J. H. Fleckenstein, N. Volze, K. Buis, R. Verhoeven, P. Meire, and O. Batelaan. 2009. Transient or steady-state? Using vertical temperature profiles to quantify groundwater–surface water exchange. Hydrological Processes 23:2165–2177.

Baraer, M., J. M. McKenzie, B. G. Mark, J. Bury, and S. Knox. 2009. Characterizing contributions of glacier melt and groundwater during the dry season in a poorly gauged catchment of the Cordillera Blanca (Peru). Advances in Geosciences 22:41–49.

Blaen, P. J., D. M. Hannah, L. E. Brown, and A. M. Milner. 2013. Water temperature dynamics in high Arctic river basins. Hydrological Processes 27:2958–2972.

Blume, T., S. Krause, K. Meinikmann, and J. Lewandowski. 2013. Upscaling lacustrine groundwater discharge rates by fiber-optic distributed temperature sensing. Water Resources Research 49:7929–7944.

Briggs, M. A., L. K. Lautz, D. K. Hare, and R. González-Pinzón. 2013. Relating hyporheic fluxes, residence times, and redox-sensitive biogeochemical processes upstream of beaver dams. Freshwater Science 32:622–641.

Briggs, M. A., L. K. Lautz, J. M. McKenzie, R. P. Gordon, and D. K. Hare. 2012. Using high-resolution distributed temperature sensing to quantify spatial and temporal variability in vertical hyporheic flux. Water Resources Research 48: W02527.

Brown, L. E., D. M. Hannah, and A. M. Milner. 2007a. Vulnerability of Alpine stream biodiversity to shrinking glaciers and snowpacks. Global Change Biology 13:958–966.

Brown, L. E., A. M. Milner, and D. M. Hannah. 2007b. Groundwater influence on alpine stream ecosystems. Freshwater Biology 52:878–890.

Brown, L. E., A. M. Milner, D. M. Hannah, C. Soulsby, A. Hodson, and M. J. Brewer. 2006. Water source dynamics in an alpine glacierized river basin (Taillon-Gabiétous, French Pyrénées). Water Resources Research 42:W08404.

Campbell, D. H., E. Muths, J. T. Turk, and P. S. Corn. 2004. Sensitivity to acidification of subalpine ponds and lakes in northwestern Colorado. Hydrological Processes 18:2817– 2834.

Casassa, G., P. López, B. Pouyaud, and F. Escobar. 2009. Detection of changes in glacial run-off in alpine basins: examples from North America, the Alps, central Asia and the Andes. Hydrological Processes 23:31–41.

Clow, D. W., L. Schrott, R. Webb, D. H. Campbell, A. Torizzo, and M. Dornblaser. 2003. Ground water occurrence and contributions to streamflow in an alpine catchment, Colorado Front Range. Groundwater 41:937–950.

Constantz, J. 2008. Heat as a tracer to determine streambed water exchanges. Water Resources Research 44:W00D10.

Cook, S. J., Z. P. Robinson, I. J. Fairchild, P. G. Knight, R. I. Waller, and I. Boomer. 2010. Role of glaciohydraulic supercooling in the formation of stratified facies basal ice: Svínafellsjökull and Skaftafellsjökull, southeast Iceland. Boreas 39: 24–38.

Cooper, R. J., J. L. Wadham, M. Tranter, R. Hodgkins, and N. E. Peters. 2002. Groundwater hydrochemistry in the active layer of the proglacial zone, Finsterwalderbreen, Svalbard. Journal of Hydrology 269:208–223.

Crossman, J., I. Boomer, C. Bradley, and A. M. Milner. 2011. Water flow dynamics of groundwater-fed streams and their ecological significance in a glacierized catchment. Arctic, Antarctic, and Alpine Research 43:364–379.

Crossman, J., C. Bradley, A. M. Milner, and G. Pinay. 2013. Influence of environmental instability of groundwater-fed streams on hyporheic fauna, on a glacial floodplain, Denali National Park, Alaska. River Research and Applications 29:548–559.

Fleckenstein, J. H., S. Krause, D. M. Hannah, and F. Boano. 2010. Groundwater-surface water interactions: new methods and models to improve understanding of processes and dynamics. Advances in Water Resources 33:1291–1295.

Goodman, K. J., M. A. Baker, and W. A. Wurtsbaugh. 2010. Mountain lakes increase organic matter decomposition rates in streams. Journal of the North American Benthological Society 29:521–529.

Goodman, K. J., M. A. Baker, and W. A. Wurtsbaugh. 2011. Lakes as buffers of stream dissolved organic matter (DOM) variability: temporal patterns of DOM characteristics in mountain stream-lake systems. Journal of Geophysical Research: Biogeosciences 116:G00N02.

Guðmundsson, M. T., A. Bonnel, and K. Gunnarsson. 2002. Seismic soundings of sediment thickness on Skeiðarársandur, SE-Iceland. Jökull 51:53–64.

Gurrieri, J. T., and G. Furniss. 2004. Estimation of groundwater exchange in alpine lakes using non-steady mass-balance methods. Journal of Hydrology 297:187–208.

Hannah, D. M., I. A. Malcolm, and C. Bradley. 2009. Seasonal hyporheic temperature dynamics over riffle bedforms. Hydrological Processes 23:2178–2194.

Hatch, C. E., A. T. Fisher, J. S. Revenaugh, J. Constantz, and C. Ruehl. 2006. Quantifying surface water–groundwater interactions using time series analysis of streambed thermal re-

cords: method development. Water Resources Research 42: W10410.
Hatch, C. E., A. T. Fisher, C. R. Ruehl, and G. Stemler. 2010. Spatial and temporal variations in streambed hydraulic conductivity quantified with time series thermal methods. Journal of Hydrology 389:276–288.
Hillel, D. 1998. Environmental soil physics. Academic Press, New York.
Hillel, D. 2004. Introduction to environmental soil physics. Pages 220–232 only. Elsevier, London, UK.
Hood, J. L., J. W. Roy, and M. Hayashi. 2006. Importance of groundwater in the water balance of an alpine headwater lake. Geophysical Research Letters 33:L13405.
Huss, M., D. Farinotti, A. Bauder, and M. Funk. 2008. Modelling runoff from highly glacierized drainage basins in a changing climate. Hydrological Processes 22:3888–3902.
IGS (Icelandic Glaciological Society). 2013. From the databases of the Icelandic Glaciological Society. Icelandic Glaciological Society, Reykjavik, Iceland.
IMO (Icelandic Meteorological Office). 2013. IMO Database. Icelandic Meteorological Office, Veðurstofa Íslands, Iceland.
Jacobsen, D., A. M. Milner, L. E. Brown, and O. Dangles. 2012. Biodiversity under threat in glacier-fed river systems. Nature Climate Change 2:361–364.
Kalbus, E., F. Reinstorf, and M. Schirmer. 2006. Measuring methods for groundwater-surface water interactions: a review. Hydrology and Earth System Sciences 10:873–887.
Keery, J., A. Binley, N. Crook, and J. W. N. Smith. 2007. Temporal and spatial variability of groundwater-surface water fluxes: development and application of an analytical method using temperature time series. Journal of Hydrology 336:1–16.
Kidmose, J., B. Nilsson, P. Engesgaard, M. Frandsen, S. Karan, F. Landkildehus, M. Søndergaard, and E. Jeppesen. 2013. Focused groundwater discharge to a eutrophic seepage lake (Lake Væng, Denmark): implications for lake ecological state and restoration. Hydrogeology Journal 21:1787–1802.
Krause, S., and T. Blume. 2013. Impact of seasonal variability and monitoring mode on the adequacy of fiber-optic distributed temperature sensing at aquifer-river interfaces. Water Resources Research 49:2408–2423.
Krause, S., T. Blume, and N. J. Cassidy. 2012. Investigating patterns and controls of groundwater up-welling in a lowland river by combining fibre-optic distributed temperature sensing with observations of vertical hydraulic gradients. Hydrology and Earth System Sciences 16:1775–1792.
Krause, S., D. M. Hannah, and T. Blume. 2011a. Heat transport patterns at pool-riffle sequences of an UK lowland stream. Ecohydrology 4:549–563.
Krause, S., D. M. Hannah, and T. Blume. 2011b. Interstitial pore-water temperature dynamics across a pool-riffle-pool sequence. Ecohydrology 4:549–563.
Krause, S., D. M. Hannah, P. J. Wood, and J. Sadler. 2011c. Hydrology and ecology interfaces: processes and interactions in wetland, riparian and groundwater-based ecosystems. Ecohydrology 4:476–480.
Langston, G., L. R. Bentley, M. Hayashi, A. McClymont, and A. Pidlisecky. 2011. Internal structure and hydrological functions of an alpine proglacial moraine. Hydrological Processes 25:2967–2982.
Langston, G., M. Hayashi, and J. W. Roy. 2013. Quantifying groundwater-surface water interactions in a proglacial moraine using heat and solute tracers. Water Resources Research 49:5411– 5426.
Lapham, W. W. 1989. Use of temperature profiles beneath streams to determine rates of vertical ground-water flow and vertical hydraulic conductivity. US Geological Survey Water Supply Paper 2337. US Geological Survey, Reston, Virginia.
Lautz, L. K. 2010. Impacts of nonideal field conditions on vertical water velocity estimates from streambed temperature time series. Water Resources Research 46:W01509.
Lowry, C. S., J. F. Walker, R. J. Hunt, and M. P. Anderson. 2007. Identifying spatial variability of groundwater discharge in a wetland stream using a distributed temperature sensor. Water Resources Research 43:W10408.
Malard, F., K. Tockner, and J. V. Ward. 1999. Shifting dominance of subcatchment water sources and flow paths in a glacial floodplain, Val Roseg, Switzerland. Arctic, Antarctic, and Alpine Research 31:135–150.
Mark, B. G. 2008. Tracing tropical Andean glaciers over space and time: some lessons and transdisciplinary implications. Global and Planetary Change 60:101–114.
Marren, P. M., and S. C. Toomath. 2013. Fluvial adjustments in response to glacier retreat: Skaftafellsjökull, Iceland. Boreas 42:57–70.
McClymont, A. F., M. Hayashi, L. R. Bentley, and J. Liard. 2012. Locating and characterizing groundwater storage areas within an alpine watershed using time-lapse gravity, GPR and seismic refraction methods. Hydrological Processes 26:1792–1804.
Meinikmann, K., J. Lewandowski, and G. Nützmann. 2013. Lacustrine groundwater discharge: combined determination of volumes and spatial patterns. Journal of Hydrology 502:202–211.
Mellina, E., R. D. Moore, S. G. Hinch, J. S. MacDonald, and G. Pearson. 2002. Stream temperature responses to clearcut logging in BC: the moderating influences of groundwater and headwater lakes. Canadian Journal of Fisheries and Aquatic Sciences 59:1886–1900.
Michel, R. L., J. T. Turk, D. H. Campbell, and M. A. Mast. 2002. Use of natural 35S to trace sulphate cycling in small lakes, Flattops Wilderness Area, Colorado, U.S.A. Water, Air and Soil Pollution: Focus 2:5–18.
Milner, A. M., L. E. Brown, and D. M. Hannah. 2009. Hydroecological response of river systems to shrinking glaciers. Hydrological Processes 23:62–77.
Milner, A. M., and G. E. Petts. 1994. Glacial rivers: physical habitat and ecology. Freshwater Biology 32:295–307.
Nolin, A. W., J. Phillippe, A. Jefferson, and S. L. Lewis. 2010. Present-day and future contributions of glacier runoff to summertime flows in a Pacific Northwest watershed: implications for water resources. Water Resources Research 46:W12509.
Piotrowski, J. A. 2007. Groundwater under ice sheets and glaciers, in glacier science and environmental change. Pages 50–60 *in* P. G. Knight (editor). Blackwell Publishing, Malden, Massachusetts.
Richards, J., R. D. Moore, and A. L. Forrest. 2012. Late-summer thermal regime of a small proglacial lake. Hydrological Processes 26:2687–2695.
Robinson, Z. P0., I. J. Fairchild, and C. Arrowsmith. 2009a. Stable isotope tracers of shallow groundwater recharge dynam-

ics and mixing within an Icelandic sandur, Skeiðarársandur. Pages 119–125 *in* D. Marks, R. Hock, M. Lehning, M. Hayashi, and R. Gurney (editors). Hydrology in mountain regions. Publication 326. International Association of Hydrological Sciences, Wallingford, UK.

Robinson, Z. P., I. J. Fairchild, and A. J. Russell. 2008. Hydrogeological implications of glacial landscape evolution at Skeiðarársandur, SE Iceland. Geomorphology 97:218–236.

Robinson, Z. P., I. J. Fairchild, and B. Spiro. 2009b. The sulphur isotope and hydrochemical characteristics of Skeiðarársandur, Iceland: identification of solute sources and implications for weathering processes. Hydrological Processes 23:2212–2224.

Rose, L., S. Krause, and N. J. Cassidy. 2013. Capabilities and limitations of tracing spatial temperature patterns by fiber-optic distributed temperature sensing. Water Resources Research 49:1741–1745.

Roy, J. W., and M. Hayashi. 2008. Groundwater exchange with two small alpine lakes in the Canadian Rockies. Hydrological Processes 22:2838–2846.

Roy, J. W., and M. Hayashi. 2009. Multiple, distinct groundwater flow systems of a single moraine-talus feature in an alpine watershed. Journal of Hydrology 373:139–150.

Roy, J. W., B. Zaitlin, M. Hayashi, and S. B. Watson. 2011. Influence of groundwater spring discharge on small-scale spatial variation of an alpine stream ecosystem. Ecohydrology 4:661–670.

Rutter, N., A. Hodson, T. Irvine-Fynn, and M. Kristensen Solås. 2011. Hydrology and hydrochemistry of a deglaciating high-Arctic catchment, Svalbard. Journal of Hydrology 410:39–50.

Sebok, E., C. Duque, J. Kazmierczak, P. Engesgaard, B. Nilsson, S. Karan, and M. Frandsen. 2013. High-resolution distributed temperature sensing to detect seasonal groundwater discharge into Lake Væng, Denmark. Water Resources Research 49:5355–5368.

Selker, J. S., L. Thévenaz, H. Huwald, A. Mallet, W. Luxemburg, N. van de Giesen, M. Stejskal, J. Zeman, M. Westhoff, and M. B. Parlange. 2006a. Distributed fiber-optic temperature sensing for hydrologic systems. Water Resources Research 42: W12202.

Selker, J., N. van de Giesen, M. Westhoff, W. Luxemburg, and M. B. Parlange. 2006b. Fiber optics opens window on stream dynamics. Geophysical Research Letters 33:L24401.

Shaw, G. D., E. S. White, and C. H. Gammons. 2013. Characterizing groundwater-lake interactions and its impact on lake water quality. Journal of Hydrology 492:69–78.

Singh, P., and L. Bengtsson. 2005. Impact of warmer climate on melt and evaporation for the rainfed, snowfed and glacierfed basins in the Himalayan region. Journal of Hydrology 300: 140–154.

Stewart, I. T. 2009. Changes in snowpack and snowmelt runoff for key mountain regions. Hydrological Processes 23:78–94.

Tague, C., and G. E. Grant. 2009. Groundwater dynamics mediate low-flow response to global warming in snow dominated alpine regions. Water Resources Research 45:W07421.

Tweed, F. S., M. J. Roberts, and A. J. Russell. 2005. Hydrologic monitoring of supercooled discharge from Icelandic glaciers. Quaternary Science Reviews 24:2308–2318.

Tyler, S. W., J. S. Selker, M. B. Hausner, C. E. Hatch, T. Torgersen, C. E. Thodal, and S. G. Schladow. 2009. Environmental temperature sensing using Raman spectra DTS fiber-optic methods. Water Resources Research 45:W00D23.

Ward, J. V., F. Malard, K. Tockner, and U. Uehlinger. 1999. Influence of groundwater on water column conditions in a glacial floodplain of the Swiss Alps. Hydrological Processes 13: 277–293.

Wessa, P. 2012. Cross Correlation Function (v1.0.8) in Free Statistics Software (v1.1.23-r7). Office for Research Development and Education. (Available from: http://www.wessa.net /rwasp_cross.wasp/).

Westhoff, M. C., T. A. Bogaard, and H. H. G. Savenije. 2011. Quantifying spatial and temporal discharge dynamics of an event in a first order stream, using distributed temperature sensing. Hydrology and Earth System Sciences 15:1945–1957.

Westhoff, M. C., H. H. G. Savenije, W. M. J. Luxemburg, G. S. Stelling, N. C. van de Giesen, J. S. Selker, L. Pfister, and S. Uhlenbrook. 2007. A distributed stream temperature model using high resolution temperature observations. Hydrology and Earth System Sciences 11:1469–1480.

Winter, T. C. 2003. The hydrology of lakes. Pages 61–78 *in* P. E. O'Sullivan and C. S. Reynolds (editors). The lakes handbook. Volume 1: limnology and limnetic ecology. Blackwell Science, Oxford, UK.